Anti-jamming Transmission in NOMA-based Satellite-enabled IoT: A Game-theoretic Framework in Hostile Environments

Chen Han, Aijun Liu, Zhixiang Gao, Kang An, Gan Zheng, *Fellow, IEEE*, and Symeon Chatzinotas, *Fellow, IEEE*

***Abstract*—Satellite-enabled internet of things (IoT) (SatIoT) has drawn increasing attentions due to the ubiquitous coverage, high capacity and massive connectivity. The inherent openness and broadcast nature of the SatIoT are vulnerable to security threats, particularly the jamming attacks for interrupting transmissions. Non-orthogonal multiple access (NOMA) scheme has the potential to be applied in anti-jamming communication for SatIoT due to the characteristic of resource sharing. The severely jammed users can get more allocated power by forming NOMA groups with other users, and both parties can improve the spectrum efficiency by frequency sharing. In this paper, we aim to improve the performance of sum rate for SatIoT under the jamming environments. An anti-jamming transmission scheme is developed by jointly considering the NOMA-based user grouping and the power allocation for each NOMA group. Specifically, the users can enhance anti-jamming performance and improve the sum rate by NOMA-based users grouping, which is formulated as an anti-jamming coalition formation game, and the equilibrium solution is proved by the exact potential game theory. Moreover, in order to further improve NOMA performance, we derive the power allocation solution for multi-user NOMA by considering the imperfect successive interference cancellation. Finally, simulation results briefly highlight some details of the proposed approaches.**

***Index Terms*—NOMA, Satellite-enabled IoT, User grouping, Power allocation, Game theory, Anti-jamming**

This paper appears in part at the International Wireless Communications and Mobile Computing Conference (IWCMC 2023), 2023, Marrakesh, Morocco.

This work was supported in part by the National Natural Science Foundation of China under Grant No. 62201593, 62171466 and 62071352, in part by the Research Program of National University of Defense Technology under Grant ZK22-08, in part by the National Key Research and Development Program of China under Grant No. 2018YFB1801103, in part by the Natural Science Foundation on Frontier Leading Technology Basic Research Project of Jiangsu Province under Grant BK20192002, in part by the R-STR-5010-00-Z SIGCOM RG of Interdisciplinary Centre for Security, Reliability and Trust, University of Luxembourg, and in part by the National Postdoctoral Program for Innovative Talents under Grant BX20200101. *(Corresponding author: Zhixiang Gao.)*

Chen Han and Kang An are with the Sixty-Third Research Institute, National University of Defense Technology, Nanjing 21007, China (e-mail: hanchen.lgd@gmail.com; ankang89@nudt.edu.cn).

Aijun Liu and Zhixiang Gao are with the College of Communications Engineering, Army Engineering University, Nanjing 210007, China (e-mail: liuaj.cn@163.com; gaozx_1996@163.com).

Gan Zheng is with the School of Engineering, University of Warwick, Coventry, CV47AL, U.K and also with the Wolfson School of Mechanical, Electrical and Manufacturing Engineering, Loughborough University, Loughborough LE113TU, U.K. (e-mail: gan.zheng@warwick.ac.uk).

Symeon Chatzinotas is with Interdisciplinary Centre for Security, Reliability and Trust, University of Luxembourg, Luxembourg, Luxembourg (e-mail: symeon.chatzinotas@uni.lu).

I. Introduction

A. Motivations

Internet of things (IoT) integrates various kinds of controllers, sensors, intelligent terminals into all aspects of life and production [1], [2]. IoT performs wireless transmission task mainly depending on terrestrial networks, such as cellular networks, Wi-Fi, and Zigbee [3]. However, in some special scenarios, the terrestrial network is difficult to provide effective support, such as marine monitoring, emergency rescue and communication countermeasure. Moreover, over 80% of the world's land and 95% of the world's oceans are not covered by the terrestrial networks [4]. In these cases, satellites are important parts of 5G heterogeneous networks [5] and satellites communication system has played significant roles [6]. How to allocate the limited resources is an important part in satellite-terrestrial networks [7], [8]. There are various satellite communication systems can provide service for the satellite-enabled IoT (SatIoT), such as Inmarsat, Iridium, Orbcomm, and Starlinks [9]. Due to the ubiquitous coverage, high capacity and massive connectivity, SatIoT has attracted growing attention in various scenarios such as marine monitoring and emergency rescue [10]–[12]. However, the functionability of SatIoT may be severely degraded due to the jamming threat such as military electronic countermeasures. As a promising technology to break the bottleneck of the orthogonal multiple access (OMA) scheme, the non-orthogonal multiple access (NOMA) can improve the communication performance with limited resource through resource sharing [13]. According to the principle of NOMA, multiple users transmit in the same time-frequency block. How to group different users together is worth studying. Due to its inherent cooperative characteristics, the NOMA scheme can be applied in the anti-jamming communication for SatIoT, specifically, the severely jammed users can get more allocated power by forming NOMA groups with other users, and both parties can improve the spectrum efficiency by frequency sharing. Therefore, this paper investigates the anti-jamming transmission scheme for NOMA-based SatIoT in the hostile environment.

B. Contributions and Organizations

In this paper, we investigate the anti-jamming transmission scheme in the NOMA-based SatIoT. The main contributions

are summarized as follows:

- A NOMA-based anti-jamming transmission scheme is proposed to improve sum rate of the SatIoT by jointly considering multi-user power allocation and NOMA users grouping.
- The power allocation (PA) approach for multi-user NOMA is first transformed into a convex optimization problem with considering the influence of imperfect SIC. Second, based on the PA approach, a NOMA-based anti-jamming coalition formation game is formulated to improve the sum rate of all users.
- The stability, optimality and complexity anlysis of the proposed scheme are given in detail. Simulation results validate the superiority of the proposed scheme compared with conventional algorithms, and the impact of key system parameters is analyzed in this paper.

The remaining of this paper is organized as follows. The related works is introduced in Section II. Section III elucidates the system model and problem formulation. The proposed NOMA-based anti-jamming transmission approach is presented in Section IV. Simulation results and discussions are shown in Section V. Finally, Section VI draws the conclusions.

II. Related Works

SatIoT is vulnerable to jamming attacks due to the inherent openness and broadcast nature. The regular and exposed satellite location increase the jamming risk as well. Thus, anti-jamming capability and adaptive communication strategy are important requirements of SatIoT users. Nowadays, anti-jamming is an important research direction in communication security, which aims to improve the reliability of communication system, so as to avoid communication interruption in the hostile environments. Based on deep reinforcement learning and Stackelberg game, the authors in [14] proposed an anti-jamming routing approach for internet of satellites to minimize routing cost under the threat of smart jammer. In [15], the authors investigated the intelligent reflecting surface assisted anti-jamming communication via reinforcement learning. In [16], an anti-jamming dynamic sub-networks formation approach was proposed to decrease the total energy consumption of all SatIoT users in the jamming environment. The authors in [17] formulated a coordination game based dynamic anti-jamming scheme to improve spectrum efficiency. In [18], the authors proposed a distributed scheme for anti-jamming resource management for internet of satellites. The authors in [19] investigated the trajectory control problem of unmanned aerial vehicles (UAV) for satellite-UAV collaborative system in the hostile environments. In [20], UAV power allocation and satellite beam-forming were joint optimized in UAV assisted satellite-enabled vehicle networks to maximize security rate. In [21], Cybertwin was introduced into integrated satellite-terrestrial vehicle networks, and the secrecy rates of satellite-to-vehicle link and the terrestrial BS-to-vehicle link were achieved. The authors of [22] investigated symbiotic security and achieved sum secrecy rate of satellite users maximization.

In OMA scheme, different users occupy different time-frequency resources. There is no interference between different users. Different from the OMA scheme, in power-domain NOMA, the signals of multiple users are superposed at the same time-frequency resource at transmitter and send to the receivers, then the successive interference cancellation (SIC) is applied to decode its signal at the receivers [23], [24], which improves spectral efficiency compared with OMA scheme. A cooperative NOMA was proposed in [25], where the user near the source served as a relaying node to help far NOMA users. In [26], a survey of NOMA technology from a grant-free connectivity perspective was provided to deal with the challenges in massive machine-type communications. In [1], the authors studied the problem to maximize the energy efficiency in an NOMA-enabled cloud network. The authors in [27] propose a spectrum-efficient approach in the NOMA-based scenario for relay transmission. In [28], the authors studied the joint allocation of time and power resource for hybrid NOMA systems. In [9], the authors integrated multi-beam satellite with NOMA in the industrial internet of things, and a QoS-guarantee power optimization was proposed to improve transmission rate. In [29], the authors analyzed the performance of down-link NOMA for low earth orbit (LEO) satellite communication system. The authors in [30] investigated the problem of user pairing and power control in the NOMA-based integrated terrestrial-satellite networks. The authors in [31]–[33] investigated the capacity, outage and error performance of NOMA scheme. Various works had integrated NOMA with other technologies such as multi-antenna transmission [34], millimeter wave communication [35], unmanned aerial vehicle communication [36]–[38], visible light communication [39], and mobile edge caching [40] for further performance improvement [41]. For instance, the authors in [36] studied the problem to improve the efficiency of UAV-assistant data collection in the NOMA-based uplink scenario. In [40], the authors investigated an uplink NOMA-based mobile-edge computing network. As for the research methods, convex optimization and game theory are widely used to exploit the potential performance for NOMA system, such as Lagrangian duality theory [42], monotonic optimization [43], and matching game [44]. In [45], the author formulated a constrained optimization problem to maximize the sum rate for a NOMA-based integrated terrestrial-satellite networks by joint beam-forming and power allocation. The authors in [46] investigated the imperfect SIC factor and decoding error of the NOMA approach, and proposed a game based algorithm for NOMA pairing. In [47], the authors exploited NOMA's specific potential in video multicast transmission by maximizing average quality of experience over all users with the basic services constraint and statistical channels considered. In [48], NOMA was applied to assisted wireless caching networks. The authors of [49] proposed a two beamforming scheme for robust NOMA transmission in SatIoT. The power optimization of age of information was investigated in [50] for NOMA-based SatIoT. In [51], the combine of NOMA and orthogonal time frequency space (OTFS) modulation was investigated in SatIoT.

A lot of interesting researches have been done on NOMA technology, but the application of NOMA technology in the field of anti-jamming is still an open topic. Due to the resource

TABLE I: Summation of Notations.

Notations	Explanation
P	Initial allocated power for each user
B	Initial allocated bandwidth for each user
P_J	Jamming power
$d_{J,i}$	The distance from the jammer's location X_J to user's location X_i
σ_0^2	Channel noise
$R_{c,i}^F$	The transmission rate of the i-th user in group Co_c with OFDMA scheme
$R_{c,i}$	The transmission rate of the i-th user in group Co_c with NOMA scheme
$R_{c,i}^\mu$	The transmission rate of the i-th user in group Co_c with NOMA scheme and imperfect SIC
N_c	The number of users in group Co_c
$h_{c,i}$	The channel quality of the i-th user in group Co_c
$a_{c,i}$	The power allocation coefficient for the i-th user in the NOMA-based group Co_c
$\mathcal{N}$	User number
$\mathcal{N}_z$	Group number
$\mathcal{C}$	Maximum number within one group
$\{Co_c\}$	The coalition scheme
μ	imperfect SIC factor

sharing between NOMA users, the severely jammed users can get more allocated power, and both users can improve the spectrum efficiency by frequency sharing, thus improving the overall communication performance. This feature fits nicely with the need of anti-jamming defense for SatIoT. However, the relevant works on combining NOMA into anti-jamming design are rare in the state-of-the-art research.

III. System Model and Problem Formulation

A. System Model

A SatIoT model is considered in this paper, which includes a multi-beam LEO satellite and numerous ground stations [16]. This paper mainly studies the downlink transmission process from satellite to the ground stations for IoT. The satellites transmit the data to the ground stations, which then transmit the information to the serving IoT terminals. The satellite can form some spot beams to serve ground stations which is referred to as users below. The total power and bandwidth used by the satellite are fixed, but the power and bandwidth used for each users can be adjusted dynamically. In the initial phase, each user is allocated the same power and frequency resources. Each user's power is P, and the allocated bandwidth is B. There is a jammer located in the target region served by the satellite. Inspired by [14], the jammer uses reinforcement learning to select the position with the best jamming benefit. Then, the jamming location can be observed by the direction finding and positioning equipment from the communication side. This process is not the key problem of this paper, which can be discussed in the future our work. We assumed the power

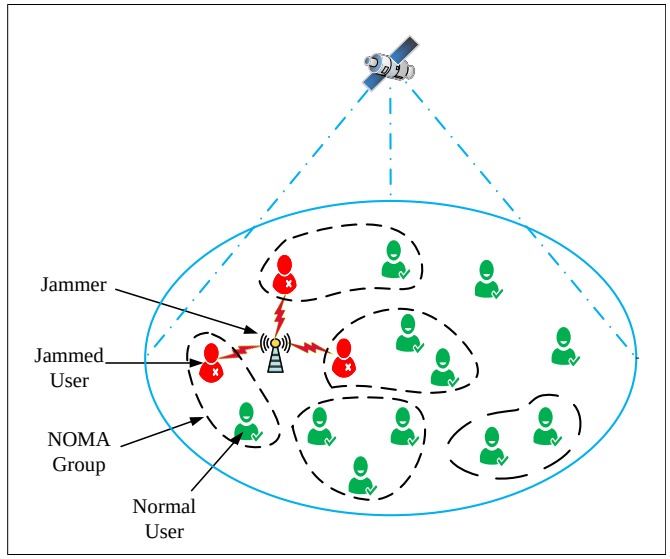

Fig. 1: System model. The satellite serves the target region, where the severely jammed users are grouped with others, and the NOMA scheme is adopted to improve the transmission rate.

suppression jammer is located the key attacking location and the jamming power $\sigma_{J,i}^2(t)$ on the i-th user is given as:

$$\sigma_{J,i}^2(t) = P_J g_i^J(t) d_{J,i}^{-2},\ d_{J,i} = \|X_J - X_i\|, \tag{1}$$

where $d_{J,i}^{-2}$ is the path loss from the jammer's location X_J to user's location X_i. P_J is the jamming power. $g_i^J(t)$ is the channel gain of the jamming link, which follows Nakagami-m fading model [52], [53]. The probability density function (PDF) of $\left|g_i^J(t)\right|^2$ is expressed as:

$$f_{\left|g_i^J(t)\right|^2}(x) = \frac{x^{\theta-1}\exp(-\frac{x}{\eta})}{\Gamma(\theta)\eta^\theta}, \tag{2}$$

where $\Gamma(\bullet)$ is the Gamma function.

As shown in Fig. 1, users form different groups for satellite spot beam transmission and the interference between different beams is assumed eliminated. If users in Co_c adopt orthogonal frequency division multiple access (OFDMA) scheme, the received signal fo the i-th user with jamming interference is expressed as:

$$y_{c,i}^F(t) = \sqrt{G_s L_i G_i P} g_{c,i}(t) s_i(t) e^{j2\pi f_d(t)t} + \sigma_0^2 + \sigma_{J,i}^2(t), \tag{3}$$

where $s_i(t)$ is the transmission signal for the i-th user, $E[\left|s_i(t)\right|^2] = 1$. G_s is the antenna gain at satellite, G_i is the antenna gain at the i-th user, $L = (c/4\pi f_c d)^{-2}$ is the free space loss, and c, f_c, d are the speed of light, carrier frequency and distance from the satellite to the user, respectively. Moreover, G_s, L_i, G_i are all constants, and thus, without loss of generality, we set $G_s L_i G_i = 1$ [19]. f_d is the Doppler shift caused by the satellite movement which is assumed to be fully compensated by carrier frequency offset and correction [54]. σ_0^2 is the channel noise. $g_{c,i}(t)$ is the channel gain of the satellite-to-ground links which follows the shadowed-Rician fading model [55], [56] and the PDF

of $|g_{c,i}(t)|^2$ is given as:

$$f_{|g_{c,i}(t)|^2}(x) = \alpha \exp(-\beta x)_1 F_1(\mathrm{m}, 1, \xi x), \tag{4}$$

where ${}_1F_1(\cdot,\cdot,\cdot)$ is the confluent hypergeometric function, $\alpha = (2\mathrm{bm}/(2\mathrm{bm}+\Omega))^{\mathrm{m}}/2\mathrm{b}$, $\beta = 1/2\mathrm{b}$, $\xi = \Omega/2\mathrm{b}/(2\mathrm{bm}+\Omega)$, and b, m, Ω are shadowing-Rician fading parameters. Hence, the transmission rate of the i-th user in group Co_c with OFDMA scheme is given by:

$$R^F_{c,i} = B\log_2(1+\frac{P\|g_{c,i}(t)\|^2}{\sigma_0^2+\sigma^2_{J,i}(t)}) = B\log_2\left(1+\frac{h_{c,i}}{N_c}\right), \tag{5}$$

where $h_{c,i} = N_c P\|g_{c,i}(t)\|^2/(\sigma_0^2+\sigma^2_{J,i}(t)), i \in [1, N_c]$ is defined as the channel quality of the i-th user, which differs from the signal to jamming plus noise ratio (SJNR) by a power allocation coefficient, $N_c = |Co_c|$ is the number of users in group Co_c.

The channel gain of users may decrease sharply due to the channel fading and malicious jamming. Thus, as shown in Fig. 1, users with different channel state attempt to improve transmission performance by user grouping. Specifically, users in the same group utilize NOMA scheme to increase the sum rate effectively. Thus, the severely jammed users can get more allocated power, and both users can improve the spectrum efficiency by frequency sharing.

In group Co_c, when NOMA scheme is adopted, the N_c users in the same group share the total frequency resource $N_c \times B$ together and redistribute the whole power $N_c \times P$. Therefore, the received signal of the i-th user in group Co_c with NOMA scheme is expressed as:

$$y^N_{c,i}(t) = g_{c,i}(t)\sum_{i=1}^{N_c}\sqrt{a_{c,i}N_c P}s_i(t) + \sigma_0^2 + \sigma^2_{J,i}(t), \tag{6}$$

where $a_{c,i}$ is the power allocation coefficient for the i-th user in the NOMA-based group Co_c, $0 < a_{c,i} < 1, \sum_{i=1}^{N_c} a_{c,i} = 1$.

For the sake of simplicity, the group Co_c with N_c users is defined as:

$$Co_c = \{h_{c,1}, h_{c,2}, \ldots, h_{c,N_c}\}, \tag{7}$$

If users in Co_c adopt NOMA scheme, the members in Co_c are arranged as:

$$h_{c,1} \le h_{c,2} \le \cdots \le h_{c,N_c}, \tag{8}$$

$$a_{c,1} \ge a_{c,2} \ge \cdots \ge a_{c,N_c}, \ \sum\nolimits_{i=1}^{N_c} a_{c,i} = 1. \tag{9}$$

According to the SIC technology, the transmission rate of the i-th user is in group Co_c given by [57]:

$$R_{c,i} = N_c B\log_2\left(1+\frac{h_{c,i}a_{c,i}}{1+h_{c,i}\sum\limits_{v=i+1}^{N_c}a_{c,v}}\right), \tag{10}$$

The sum rate of all users ($N \ge 2$) in Co_c is :

$$C^S_{N_c} = N_c B\sum_{i=1}^{N_c}\log_2\left(1+\frac{h_{c,i}a_{c,i}}{1+h_{c,i}\sum\limits_{v=i+1}^{N_c}a_{c,v}}\right). \tag{11}$$

As remarked in [57], two-user NOMA is the optimal NOMA pairing. It is true only if a user with lower channel quality is added into the NOMA group without bring more resource. On the contrary, the sum rate increases, if the new added user has better channel quality, which is shown in the conclusion in **Appendix A**.

Furthermore, by further considering the imperfect SIC, the signals that are not fully decoded become interference to the later signals. Hence, the i-th user's transmission rate in group Co_c is given by:

$$R^\mu_{c,i} = N_c B\log_2\left(1+\frac{h_{c,i}a_{c,i}}{1+h_{c,i}(\sum\limits_{v=1}^{i-1}\mu_v a_{c,v}+\sum\limits_{v=i+1}^{N_c}a_{c,v})}\right), \tag{12}$$

where $\mu_v \in [0,1]$ characterizes the error propagation caused by imperfect SIC [58]. As the number of users increases, the SIC process increases the receiver's complexity dramatically. As indicated in Eq. (12), due to the imperfect SIC, the intra-user interference can gradually become intolerable, and damage the system performance. Therefore, in this paper, there is a maximum number of users within one group, i.e., $|Co_c| \le \mathcal{C}$.

B. Problem Formulation

The problem investigated in this paper is to maximize the sum rate of all users by NOMA-based grouping and corresponding power allocation under the threat of jamming attacks:

$$P1: \max_{\{Co_c\}_{c=1}^{\mathcal{N}_z}}\left\{\sum_{c=1}^{\mathcal{N}_z}\max_{\{a_{c,i}\}_{i=1}^{N_c}}\left\{\sum_{i=1}^{N_c}R^\mu_{c,i}\right\}\right\}, \tag{13}$$

$$s.t. \quad \text{Eq. (8), (9), (12)}, \tag{13a}$$

$$R^\mu_{c,i} \ge R^F_{c,i}, \forall i, \forall c, \tag{13b}$$

$$|Co_c| \le \mathcal{C}, \forall c, \tag{13c}$$

$$\bigcup_{c\in[1,\mathcal{N}_z]} Co_c = \left[h_{1,1}, h_{1,2}, \ldots, h_{c,i}\ldots, h_{\mathcal{N}_z,N_{\mathcal{N}_z}}\right]. \tag{13d}$$

where where $\mathcal{N}_z$ is the group number. Eq. (13b) ensures the minimal QoS requirement of each user, which is set according to OFDMA scheme based on Eq. (5). Eq. (13d) ensures that the groups cover all users. Note that the channel quality of the users can be influenced by the distance between the satellite and the users or the distance between the users and the jammer, the final result of problem $P1$ may accordingly change with the motion of the satellite and the jammer.

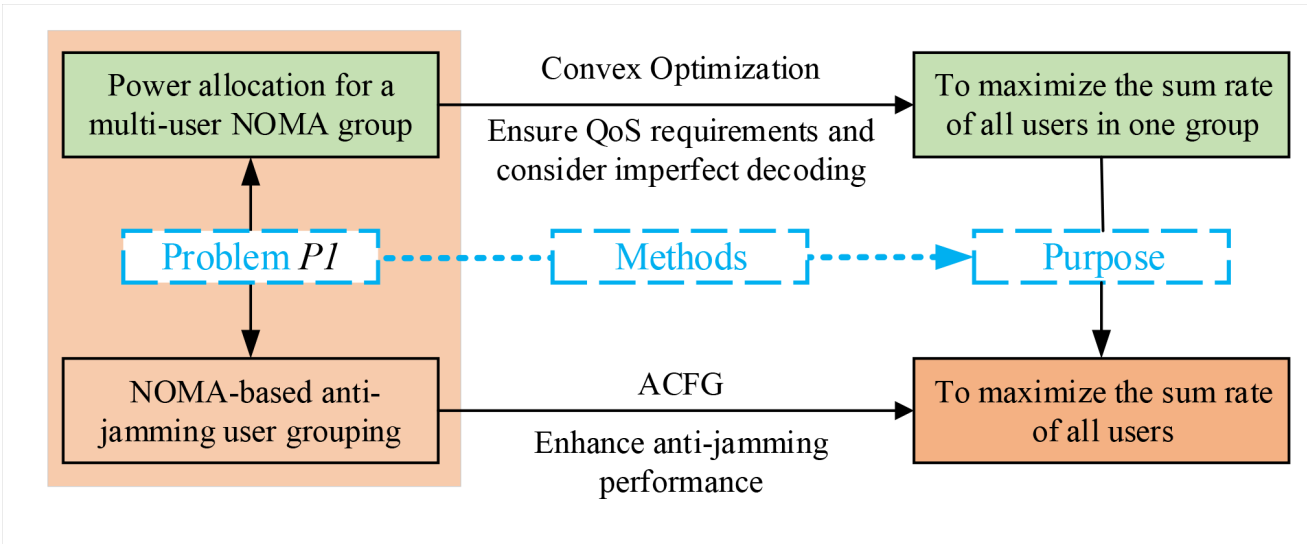

Fig. 2: NOMA-based anti-jamming transmission framework.

IV. NOMA-Based Anti-jamming Transmission Scheme

As shown in Fig. 2, the problem $P1$ is divided into two parts to solve: power allocation for a multi-user NOMA group and NOMA-based anti-jamming user grouping. Firstly, in order to break the two-user limit and further improve the NOMA performance, the power allocation problem for multi-user NOMA group is solved through convex optimization for maximizing the sum rate of all users in one group, while considering the influence of imperfect decoding and ensuring the QoS requirement of each user; Secondly, NOMA-based users grouping problem is addressed to maximize all users' sum rate via the anti-jamming coalition formation game (ACFG) with consideration of the anti-jamming requirements of each user.

A. Power allocation for a multi-user NOMA group

To maximize the sum rate of all users, the power allocation problem for multi-user NOMA group needs to be solved firstly. The maximal sum rate of all users in Co_c is defined as $\mathbb{R}_c$,

$$\mathbb{R}_c = \arg \max_{\{a_{c,i}\}_{i=1}^{N_c}} \sum_{i=1}^{N_c} R_{c,i}^{\mu}, \tag{14}$$
$$s.t. \text{ Eq. (13a), (13b), (13c).}$$

According to [59], Eq. (13b) is non-convex, and (14) is a non-convex problem. Next, we can take an iteration-based method to convert it into a convex optimization problem. For the sake of simplicity, the subscript c of the channel quality $h_{c,i}$ and the power allocation coefficient $a_{c.i}$ are omitted in the rest paper.

According to Eq. (12), the transmission rate of the i-th user $(2 \leq i \leq N_c - 1)$ is,

$$R_{c,i}^{\mu} = N_c B \log_2 \left(1 + \frac{h_i a_i}{1 + h_i \left(\sum_{v=1}^{i-1} \mu_v a_v + \sum_{v=i+1}^{N_c} a_v \right)} \right) \tag{15}$$
$$= N_c B \log_2 \left(1 + h_i \left(\sum_{v=1}^{i-1} \mu_v a_v + \sum_{v=i}^{N_c} a_v \right) \right) - \tag{15a}$$
$$N_c B \log_2 \left(1 + h_i \left(\sum_{v=1}^{i-1} \mu_v a_v + \sum_{v=i+1}^{N_c} a_v \right) \right). \tag{15b}$$

Then, by the first-order Taylor expansion for multivariate function at the points of $[a_1^r, a_2^r, \ldots a_{N_c}^r]$, the Eq. (15b) is rewritten as [60]:

$$\hat{R}_i = N_c B \log_2 \left(1 + h_i \left(\sum_{v=1}^{i-1} \mu_v a_v + \sum_{v=i+1}^{N_c} a_v \right) \right) \tag{16}$$
$$= N_c B \log_2 \left(1 + h_i \sum_{v=1}^{N_c} \mu_v \eta_v a_v \right)$$
$$\leq N_c B \sum_{v=1}^{N_c} X_{i,v}^r \left(a_v - a_v^r \right) + Q_i^r \triangleq \widetilde{R_i} \tag{17}$$
$$s.t. \ \eta_v = 1, v \in [1, i-1], \eta_v = 1/\mu_v, v \in [i+1, N_c], \eta_i = 0,$$

where a^r is the power allocation coefficient in the r-th iteration, and X_i^r and Q_i^r are given as follows,

$$X_{i,v}^r = \frac{h_i \mu_v \eta_v \log_2(e)}{1 + h_i \sum_{x=1}^{N_c} \mu_v \eta_v a_x^r}, \tag{18}$$

$$Q_i^r = N_c B \log_2 \left(1 + h_i \sum_{v=1}^{N_c} \mu_v \eta_v a_v^r \right), \tag{19}$$
$$s.t. \ \eta_v = 1, v \in [1, i-1], \eta_v = 1/\mu_v, v \in [i+1, N_c], \eta_i = 0.$$

Then, Eq. (15) becomes convex as [1]:

$$\widetilde{R_{c,i}^{\mu}} = N_c B \log_2 \left(1 + h_i \left(\sum_{v=1}^{i-1} \mu_v a_v + \sum_{v=i}^{N_c} a_v\right)\right) - \widetilde{R_i}. \tag{20}$$

Thus, the power allocation problem in (14) is newly formulated as:

$$\mathbb{R}_c^{'} = \arg \max_{\{a_i\}_{i=1}^{N_c}} \sum_{i=1}^{N_c} \widetilde{R_{c,i}^{\mu}}, \tag{21}$$

$$s.t. \text{ Eq.(13a), (13c)}, \tag{21a}$$

$$\widetilde{R_{c,i}^{\mu}} \geq R_{c,i}^{F}, \forall i, \forall c. \tag{21b}$$

where $R_{c,i}^{F}$ is a constant. Thus, (21) is convex and it can be solved by CVX. According to Eq. (16) and (17), the result $\mathbb{R}_c^{'}$ is the lower-bound of the result $\mathbb{R}_c$ in each iteration. Therefore, the optimal $\mathbb{R}_c^*$ of the original non-convex problem (14) can be obtained by solving convex problem (21) with finite iterations.

B. NOMA-based anti-jamming user grouping

Based on the convex optimization and iterative solution in III.A, we can get the maximal sum rate of all users in Co_c, i.e., $\mathbb{R}_c^*$, and $P1$ is simplified as:

$$P1' : \max_{\{Co_c\}_{c=1}^{\mathcal{N}_z}} \sum_{c=1}^{\mathcal{N}_z} \mathbb{R}_c^*, \tag{22}$$

$$s.t. \quad \text{Eq. (13c)}.$$

Next, we investigate the NOMA-based user grouping strategy to solve (22). This paper formulates the user grouping problem in the jamming environment as an ACFG, and proposes a distributed NOMA-based anti-jamming coalition formation algorithm to divide users into several coalitions. In this case, the NOMA approach can effectively improve the transmission rate of the jammed users under the premise of guaranteeing the QoS of other users in the same coalition, thus further improving the sum rate of all users. Firstly, we define the ACFG as follows.

Definition 1: (ACFG): All users can be divided into several non-overlapping NOMA-based coalitions $\{Co_c\}_{c=1}^{\mathcal{N}_z}$, $\bigcup_{c=1}^{\mathcal{N}_z} Co_c = \left[h_{1,1}, h_{1,2}, \ldots, h_{c,i} \ldots, h_{\mathcal{N}_z, N_{\mathcal{N}_z}}\right]$. Each user has its own coalition preference order and coalition change principle. Then the grouping strategy $\{Co_c\}_{c=1}^{\mathcal{N}_z}$ constitutes the ACFG.

For notation simplification, i is used to represent the i-th member in Co_c, and define the game utility of each user as follows:

$$u_i = \mathcal{R}(Co_c) - \mathcal{R}(Co_c \backslash i), \tag{23}$$
$$\forall i \in Co_c, \forall c,$$

where $\mathcal{R}(Co_c) = \mathbb{R}_c^* = \arg \max_{\{a_i\}_{i=1}^{N_c}} \sum_{i=1}^{N_c} R_{c,i}^{\mu}$ is the maximum sum rate of all users in Co_c, and $\mathcal{R}(Co_c \backslash i)$ is the maximum sum rate of $\{Co_c \backslash i\}$, i.e., the maximum sum rate except the i-th user in Co_c. Note that $\{Co_c\}$ and $\{Co_c \backslash i\}$ are the different coalitions with different NOMA pairing. Then, u_i is defined to depict the contribution of the i-th user for coalition Co_c, which represents a mapping relationship from the individual to the whole.

The coalition preference order determines whether users are caning to deviate from or join in this coalition, and affects the convergence and stability of the ACFG. This paper proposes a partial order to increase the sum rate of all coalitions and attempt to obtain a better solution towards optimal solution via a distributed way.

Definition 2: (Partial Order): If the user $i \in Co_{c'}$ and the coalition $\{Co_c, Co_{c'}\}$, $c, c' \in [1, \mathcal{N}_z]$ satisfy Eq. (24), the partial order in ACFG is performed:

$$\begin{aligned} Co_c \succ_i Co_{c'} &\Leftrightarrow u_i\left(Co_c \cup i\right) > u_i\left(Co_{c'}\right) \\ &\Leftrightarrow \mathcal{R}(Co_c \cup i) - \mathcal{R}(Co_c) > \mathcal{R}(Co_{c'}) - \mathcal{R}(Co_{c'} \backslash i) \\ &\Leftrightarrow \mathcal{R}(Co_c \cup i) + \mathcal{R}\left(Co_{c'} \backslash i\right) > \mathcal{R}(Co_c) + \mathcal{R}(Co_{c'}). \end{aligned} \tag{24}$$

The coalition change principle is the way to change the current coalition. In this paper, we propose a capped split-merge principle. Users can maximize their game utilities by splitting or merging to leave the old coalition or join a new one.

Definition 3: (Capped Split-Merge Principle): If user i can get a higher game utility, i can deviate from the current coalition $Co_{c'}$ and join in the new coalition Co_c,

$$\begin{aligned} i \rightarrow Co_c \Rightarrow &\{Co_c \cup i\} \wedge \{Co_{c'} \backslash i\} \\ \Leftrightarrow &u_i\left(Co_c \cup i\right) > u_i\left(Co_{c'}\right). \end{aligned} \tag{25}$$

In addition, there is a special case: user i can leave $Co_{c'}$ and form a new one that includes only itself, i.e., $Co_c = \{i\}$,

$$\begin{aligned} i \rightarrow \{i\} \Rightarrow &\{i\} \wedge \{Co_{c'} \backslash i\} \Leftrightarrow u_i(i) > u_i\left(Co_{c'}\right) \\ \Leftrightarrow &\mathcal{R}(i) + \mathcal{R}\left(Co_{c'} \backslash i\right) > \mathcal{R}(Co_{c'}). \end{aligned} \tag{26}$$

According to the partial order and capped split-merge principle, each user's coalition altering can further increase the sum rate of both the old coalition $Co_{c'}$ and new coalition Co_c. It can simultaneously increase the sum rate of all the coalitions. Then, based on ACFG, a NOMA-based anti-jamming coalition formation algorithm (NACF) is proposed to improve sum rate of all users by anti-jamming user grouping, which is elaborated in Algorithm 1.

C. Algorithm Analysis

The stability, optimality and complexity of the proposed scheme are discussed as follows.

1) Stability analysis:

Definition 4: (Stable Coalition Formation): If no user can unilaterally increase the game utility by adjusting its own policy, the current coalition formation $\{Co_c\}_{c=1}^{\mathcal{N}_z}$ is stable.

$$\begin{aligned} &u_i\left(Co_c, Co_{-c}\right) \geq u_i\left(Co_{c'}, Co_{-c'}\right) \\ &\forall i \in Co_c, \ Co_c \neq Co_{c'}, \ \forall c. \end{aligned} \tag{27}$$

Theorem 1: If partial order is performed, the proposed ACFG can converge to a stable coalition formation.

Proof: According to Definition 2, if all users choose coalitions according to the partial order, each user's coalition

[1]For the case of $i = 1$ and $i = N_c$, we can obtain the similar results.

Algorithm 1: The NOMA-based anti-jamming coalition formation algorithm (NACF)

Input: All the users, $i \in [1, \mathcal{N}]$, and the sets of adjacent users for each i that meet the distance requirement L_{th}, i.e., $A_i = \{j \mid d_{i,j} < L_{th}, i, j \in [1, \mathcal{N}]\}$

Output: The coalition formation scheme $\{Co_c\}_{c=1}^{\mathcal{N}_z}$.

Initialize the coalitions, and each user individually forms a coalition, i.e., $i \to Co_{c'}$, $Co_{c'} = \{i\}$. For each user i, record its current coalition $Co_{c'}$ and the corresponding game utility $u_{c'}^i$.

for slot t=1 **to** T **do**

  Each user i chooses a user j from A_i in turn, and tries to join in the new coalition Co_c which j belongs to, i.e., $i \to Co_c \Rightarrow \{Co_c \cup i\} \wedge \{Co_{c'} \backslash i\}$.

  According to Eq. (25), i steps into the coalition Co_c, and measures the new utility u_c^i.

  According to Eq. (24), i determines the final coalition, i.e., if $u_c^i > u_{c'}^i$, i finally deviates from the old coalition $Co_{c'}$ and joins in the new coalition Co_n.

  $t \leftarrow t + 1$.

end

change only increases the sum rate of the old and new coalitions. Thus, the sum rate of all coalitions can continually increase with user's selection. Meanwhile, the available coalition selection and achieved sum rate are limited. Thus, the total sum rate can increase to the maximum, and the coalition formation result is finally steady.

If users finally obtain an unstable coalition formation result $\{Co_c\}^*$, there must be users changing coalition according to Definition 3. The sum rate of the whole system can further increase, which is contrary to the finite utility limited by the available resource and user number. Therefore, the coalition formation can finally be stable. ■

2) Optimality analysis:

The exact potential game (EPG) is developed to demonstrate the optimality of the obtained stable coalition formation.

Definition 5: (EPG): If there exists a potential function ϕ, which meets Eq. (28), this game model is an EPG:

$$\phi_i\left(Co_c\right) - \phi_i\left(Co_{c'}\right) = u_i\left(Co_c\right) - u_i\left(Co_{c'}\right), \forall c. \tag{28}$$

Theorem 2: If Eq. (23) is set as the utility function, the proposed ACFG is an EPG. Then, there exists one Nash equilibrium (NE) point at least, which is a sub-optimal solution as well.

Proof: Define the potential function as $\phi = \sum_{c=1}^{\mathcal{N}_z} \mathbb{R}_c^*$, which is the total sum rate of all the users. When the user i leaves $Co_{c'}$ and steps into Co_c, the increment of ϕ is:

$$\begin{aligned} &\phi_i\left(Co_c\right) - \phi_i\left(Co_{c'}\right) \\ =&\mathcal{R}\left[Co_c \cup i\right] + \mathcal{R}\left[Co_{c'} \backslash i\right] \\ &+ \mathcal{R}\left[\{Co_c\}_{c=1}^{\mathcal{N}_z} \backslash \{Co_c \cup i\} \backslash \{Co_{c'} \backslash i\}\right] \\ &- \mathcal{R}\left[Co_c\right] - \mathcal{R}\left[Co_{c'}\right] - \mathcal{R}\left[\{Co_c\}_{c=1}^{\mathcal{N}_z} \backslash Co_c \backslash Co_{c'}\right] \\ =&\mathcal{R}\left[Co_c \cup i\right] - \mathcal{R}\left[Co_c\right] - \left(\mathcal{R}\left[Co_{c'}\right] - \mathcal{R}\left[Co_{c'} \backslash i\right]\right). \end{aligned} \tag{29}$$

Since user's coalition change only affects the sum rate of the previous coalition $Co_{c'}$ and the current new coalition Co_c. The sum rate of other coalitions can not be affected. Thus, $\mathcal{R}\left[\{Co_c\}_{c=1}^{\mathcal{N}_z} \backslash \{Co_c \cup i\} \backslash \{Co_{c'} \backslash i\}\right]$ is equal to $\mathcal{R}\left[\{Co_c\}_{c=1}^{\mathcal{N}_z} \backslash Co_c \backslash Co_{c'}\right]$.

Meanwhile, the increment of utility function is:

$$\begin{aligned} &u_i\left(Co_c\right) - u_i\left(Co_{c'}\right) = \\ &\mathcal{R}\left[Co_c \cup i\right] - \mathcal{R}\left[Co_c\right] - \left(\mathcal{R}\left[Co_{c'}\right] - \mathcal{R}\left[Co_{c'} \backslash i\right]\right). \end{aligned} \tag{30}$$

Therefore, the proposed ACFG satisfies Eq. (28) and it is an EPG.

Based on [16], EPG has one NE point at least, and the globally optimal solution is also an NE point. Thus, if Eq. (23) is set as the game utility function, users can achieve a stable coalition formation, and the corresponding sum rate of all users approximately converges to the sub-optimal solution. ■

3) Complexity analysis:

Since the proposed NACF algorithm is a distributed algorithm based on ACFG, each user is able to optimize their own strategy of coalition selection independently. Therefore, in the proposed NACF algorithm, the computational complexity of each user is mainly reflected in the coalition change when the user interacts with the limited adjacent users at every slot. Each user interacts with a maximum of $|A_i|$ users at a time, so the scalar multiplication cost is $\mathcal{O}\left(T\left|A_i\right|\right)$ during T slots, where $|A_i|$ is the number of adjacent users of user i. Compared with the centralized matching approach [61] and Hungarian algorithm-based user grouping approach [62], whose scalar multiplication cost are $\mathcal{O}\left(M^2\right)$ and $\mathcal{O}\left(M^3\right)$, where M is the total number of users, $M \gg |A_i|$. Thus, the proposed NACF scheme has significantly lower computational complexity, especially as the number of users increases dramatically.

V. Simulation Results

In this section, simulation results are provided to validate the superiority of the proposed scheme. Specifically, the simulation parameters are given in TABLE II and III [56].

The users' location is shown in Fig. 3(a), and the user's channel quality is shown in Fig. 3(b). It is indicated that the location and jamming have significant impact on user's channel quality. Users that are closed to the jammer have worse channel qualities. The influence of the jamming signal reduces as the distance increases.

The coalition formulation result obtained by the proposed NACF algorithm is shown in Fig. 4(a). Obviously, heavily

TABLE II: The parameters of Shadowed-Rician model and Nakagami-m model

Shadowed-Rician model	b	m	Ω	Nakagami-m model	θ	η
Heavy shadowing	0.063	0.739	8.97×10^{-4}	Heavy jamming	4	2
Average shadowing	0.126	10.1	0.835	Average jamming	3	1
Light shadowing	0.79	97	6.45	Light jamming	1	1

TABLE III: Simulation parameters.

Parameters	Value
Initial allocated power for each user	$P = 1$W
Initial allocated bandwidth for each user	$B = 2$MHz
Jamming power	$P_J = 1$W
Channel noise	$\sigma^2 = 0.01$
User number	$\mathcal{N} = 16$
Maximum number within one group	$\mathcal{C} = 3$
imperfect SIC factor	$\mu = 0.05$

jammed users need to form coalition with users farther away from the jammer for better anti-jamming defense. When the attack location of jammer changes from Fig. 4(a) to Fig. 4(b), the coalition formation results adjusted by the users is shown in Fig. 4(b). Compared with Fig. 4(a), more users change their coalition selection due to the closer jamming location. The comparison results demonstrate the dynamic adaptability of the proposed scheme to jamming attacks.

The coalition formation process is shown in Fig. 5. As the iteration increases, the sum rate of all the users increases, and finally converges to a stable point. It is consistent with the Theorem 1.

As shown in Fig. 6, the sum rate of all users gradually decreases as the increasing of jamming power. But the proposed NOMA based transmission scheme has better performance than the OMA scheme (OFDMA) in [38], the matching based scheme [61] and the Hungarian algorithm scheme in [62].

The comparison of coalition formation order is indicated in Fig. 7. Based on the proposed partial order, users can obtained a higher sum rate compared with the selfish order or strict Pareto order which are used in [63]. As proved theoretically in Theorem 2, the proposed coalition order enables users to improve their utilities by changing coalition choices, thus further increasing the overall sum rate of all users.

As shown in Fig. 8, when the coalition member limitation is $\mathcal{C} = 2$, the proposed scheme has similar performance to the matching game based approach and Hungarian algorithm. While the proposed NACF scheme has better performance than the OMA scheme, the matching game based scheme and the Hungarian algorithm scheme with $\mathcal{C} > 2$. In addition, as $\mathcal{C}$ increases, the new added users bring more resources to be allocated, thus the sum rate gradually increases. However, limited by the influence of incomplete decoding and the restriction of each user's utility, there is limited performance improvement as $\mathcal{C}$ increases.

The influence of the imperfect SIC factor μ is indicated in Fig. 9. The performance of the proposed NACF algorithm decreases as the increasing of μ. However, the performance

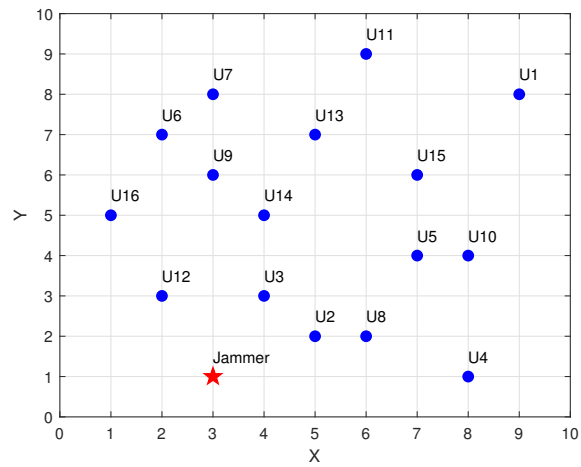

(a)

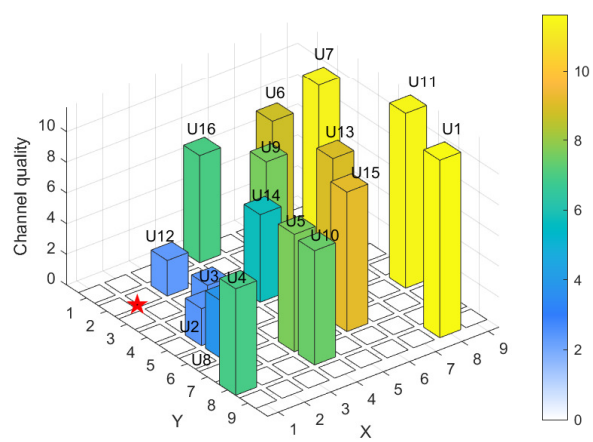

(b)

Fig. 3: (a) The location of 16 users and jammer, where the red star is the jammer's location and the blue points are the users' location; (b) The users' channel qualities.

of NACF algorithm is still better than that of the benchmark algorithms. The increasing of the imperfect SIC factor can reduce the desire to form a coalition among users, and can gradually change to a single-user coalition which eventually degenerates a full OFDMA solution. However, if users insist on using the NOMA scheme in this case, the system performance can be greatly reduced due to the intolerable imperfect SIC factor. Overall, Fig. 9 indicates the superiority on flexibility and adaptability of the proposed algorithm.

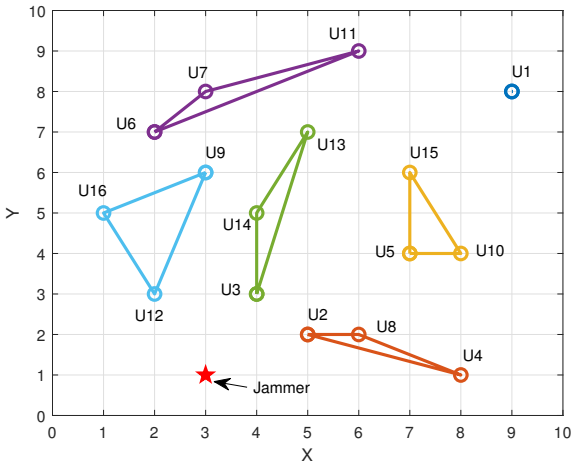

(a)

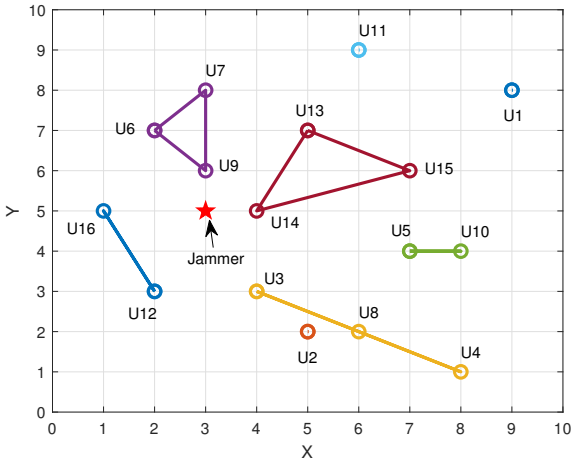

(b)

Fig. 4: (a) The coalition result, $\mu = 0.05,\ \mathcal{C} = 3,\ L_{th} = L_z/4$, where L_z is the side length of the target region. These users form 6 coalitions, and there is a coalition within only one user (the 1-th user); (b) The adjusted coalition results as jammer changing its attack location.

VI. Conclusion

In this paper, we investigated the problem of NOMA-based anti-jamming transmission scheme in SatIoT by jointly considering multi-user power allocation and NOMA users grouping in the jamming environments. Specifically, we analyzed the power allocation problem of multi-user NOMA considering the imperfect decoding at first. Secondly, an ACFG based anti-jamming user grouping algorithm was proposed to improve the sum rate of all users under the jamming threat. Finally, the stability, optimality and complexity analysis of the proposed scheme were given in detail. Simulation results were shown to validate the superior performance of the proposed approaches over conventional algorithms. Based on the proposed scheme, the severely jammed users can get more allocated power by forming NOMA groups with other users farther away from the jammer, and both parties can improve the spectrum efficiency by frequency sharing. In addition, the proposed scheme has

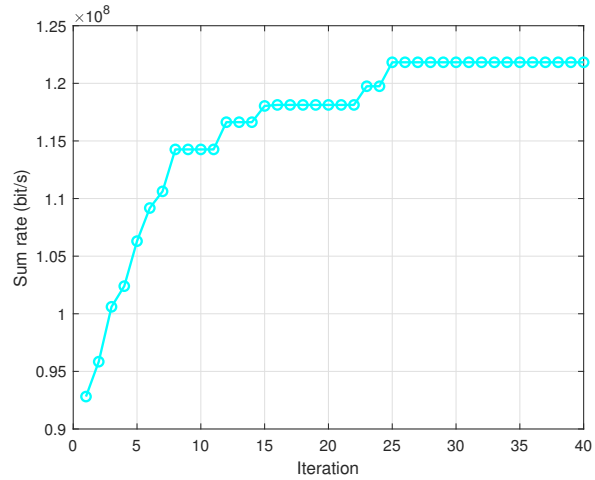

Fig. 5: The changing of sum rate during the coalition forming process in Fig. 4(a).

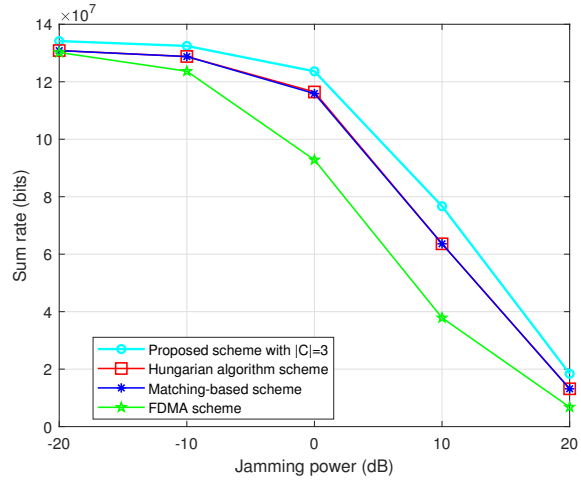

Fig. 6: The influence of jamming power, with $\mathcal{C} = 3,\ L_{th} = L_z$.

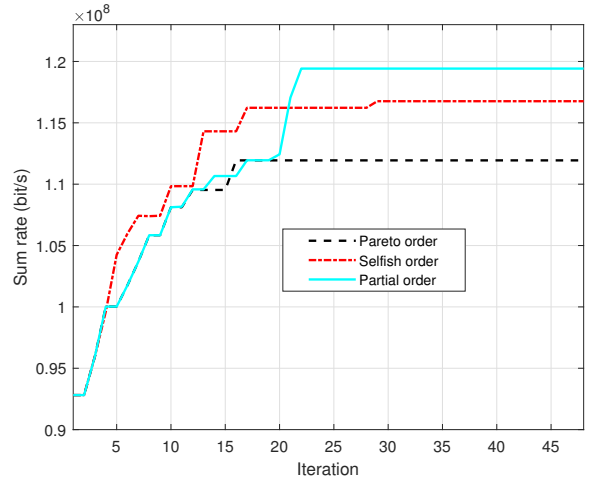

Fig. 7: The comparison between the proposed partial order and Pareto order and selfish order, with $\mu = 0.05,\ \mathcal{C} = 3,\ L_{th} = L_z/4$.

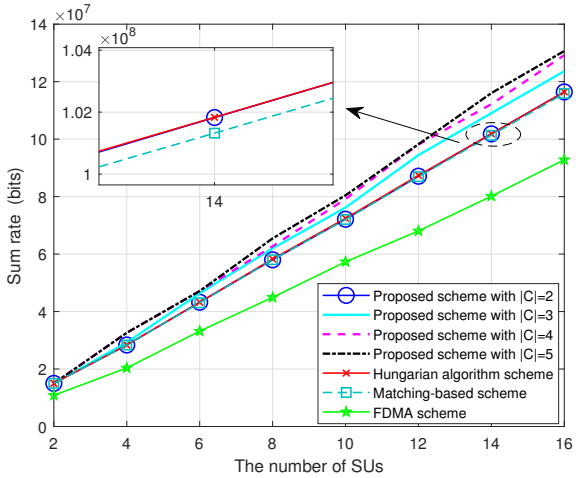

Fig. 8: The comparison between the proposed scheme, OFDMA scheme, Hungarian algorithm schem and matching game based scheme, with $\mu = 0.05,\ L_{th} = L_z$.

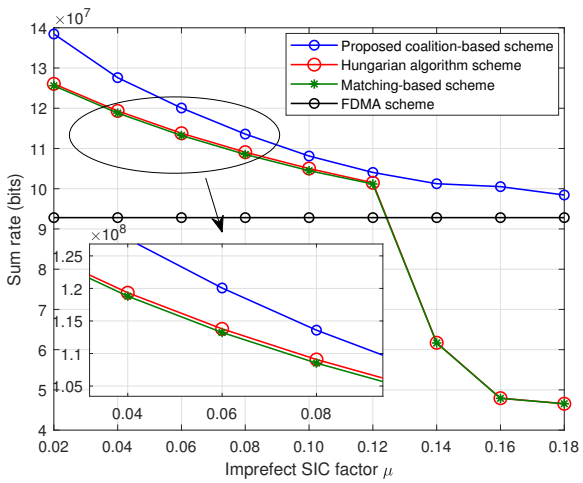

Fig. 9: The influence of imperfect SIC factor μ, with $\mathcal{C} = 3,\ L_{th} = L_z$.

better adaptability and flexibility towards imperfect SIC and jamming attacks.

Appendix A

Assuming that there are M users in group Co, $h_1 \leq h_2 \leq \ldots \leq h_M$, accordingly, power allocation coefficients are defined as $a_1 \geq a_2 \geq \ldots \geq a_M$, and the bandwidth is set as $B = 1/M$. Then, a new user with better channel quality is admitted $h_M \leq h_{M+1}$. The corresponding adjusted power coefficient is $b_1 \geq b_2 \geq \ldots \geq b_M \geq b_{M+1}$, where $b_i \leq a_i, i \in [1, M]$. The sum rate of the NOMA system with the first M users are given by:

$$C_M^S = \log_2\left(\frac{1+h_1}{1+h_1\sum\limits_{i=2}^{M} a_i}\right) + \log_2\left(1+a_M h_M\right) + \sum_{m=2}^{M-1}\log_2\left(\frac{1+h_m\sum\limits_{i=m}^{M} a_i}{1+h_m\sum\limits_{i=m+1}^{M} a_i}\right). \tag{31}$$

The sum rate with $M+1$ users is given by:

$$\begin{aligned} C_{M+1}^S = {} & \frac{M+1}{M}\log_2\left(\frac{1+h_1}{1+h_1\sum\limits_{i=2}^{M+1} b_i}\right) \\ & + \frac{M+1}{M}\log_2\left(1+b_{M+1}h_{M+1}\right) \\ & + \frac{M+1}{M}\sum_{m=2}^{M-1}\log_2\left(\frac{1+h_m\sum\limits_{i=m}^{M+1} b_i}{1+h_m\sum\limits_{i=m+1}^{M+1} b_i}\right) \\ & + \frac{M+1}{M}\log_2\left(\frac{1+h_M\sum\limits_{i=M}^{M+1} b_i}{1+h_M b_{M+1}}\right). \end{aligned} \tag{32}$$

The difference between Eq. (32) and (31) is given in Eq. (33), which is on the top of the next page. Due to $\left(\sum\limits_{i=2}^{M} a_i - \sum\limits_{i=2}^{M+1} b_i\right)(h_1 - h_2) = (b_1 - a_1)(h_1 - h_2) \geq 0$, thus, $I_1 \geq 1$. Similarly, $I_2 \geq 1$ and $I_3 \geq 1$, finally, $C_{M+1}^S - C_M^S > 0$. With the same resources, if new users with better channel qualities are added, the sum rate can increase. However, due to the restrictions of each user's QoS, as well as the constraints of imperfect SIC factor and the complexity of the receiver, the number of users cannot increase continuously.

References

[1] W. Hao, Z. Chu, F. Zhou, S. Yang, G. Sun, and K.-K. Wong, "Green Communication for NOMA-Based CRAN," *IEEE Internet Things J.*, vol. 6, no. 1, pp. 666–678, Feb. 2019.

[2] M. Liu, K. Yang, N. Zhao, Y. Chen, H. Song, and F. Gong, "Intelligent Signal Classification in Industrial Distributed Wireless Sensor Networks Based Industrial Internet of Things," *IEEE Trans. Ind. Inform.*, vol. 17, no. 7, pp. 4946–4956, Jul. 2021.

[3] X. Liu and X. Zhang, "Rate and Energy Efficiency Improvements for 5G-Based IoT With Simultaneous Transfer," *IEEE Internet Things J.*, vol. 6, no. 4, pp. 5971–5980, Aug. 2019.

[4] K. Xue, W. Meng, S. Li, D. S. L. Wei, H. Zhou, and N. Yu, "A Secure and Efficient Access and Handover Authentication Protocol for Internet of Things in Space Information Networks," *IEEE Internet Things J.*, vol. 6, no. 3, pp. 5485–5499, Jun. 2019.

[5] Y. Xu, G. Gui, H. Gacanin, and F. Adachi, "A Survey on Resource Allocation for 5G Heterogeneous Networks: Current Research, Future Trends, and Challenges," *IEEE Commun. Surv. Tutor.*, vol. 23, no. 2, pp. 668–695, Secondquarter 2021.

[6] Z. Lin, M. Lin, T. de Cola, J.-B. Wang, W.-P. Zhu, and J. Cheng, "Supporting IoT With Rate-Splitting Multiple Access in Satellite and Aerial-Integrated Networks," *IEEE Internet Things J.*, vol. 8, no. 14, pp. 11 123–11 134, Jul. 2021.

$$
\begin{aligned}
\Delta &= C_{M+1}^{S} - C_{M}^{S} \qquad (33)\\
&> \log_2\left(\frac{1+h_1}{1+h_1\sum\limits_{i=2}^{M+1} b_i}\right) + \log_2\left(1+b_{M+1}h_{M+1}\right) + \sum_{m=2}^{M-1}\log_2\left(\frac{1+h_m\sum\limits_{i=m}^{M+1} b_i}{1+h_m\sum\limits_{i=m+1}^{M+1} b_i}\right) + \log_2\left(\frac{1+h_M\sum\limits_{i=M}^{M+1} b_i}{1+h_M b_{M+1}}\right) - C_M^S\\
&= \log_2\left(\frac{1+h_1}{1+h_1\sum\limits_{i=2}^{M+1} b_i}\frac{1+h_1\sum\limits_{i=2}^{M} a_i}{1+h_1}\right) + \sum_{m=2}^{M-1}\log_2\left(\frac{1+h_m\sum\limits_{i=m}^{M+1} b_i}{1+h_m\sum\limits_{i=m+1}^{M+1} b_i}\frac{1+h_m\sum\limits_{i=m+1}^{M} a_i}{1+h_m\sum\limits_{i=m}^{M} a_i}\right)\\
&\quad + \log_2\left(\frac{1+h_M\sum\limits_{i=M}^{M+1} b_i}{1+h_M b_{M+1}}\frac{1+h_{M+1}b_{M+1}}{1+h_M a_M}\right)\\
&= \log_2\left(\frac{1+h_1\sum\limits_{i=2}^{M} a_i}{1+h_1\sum\limits_{i=2}^{M+1} b_i}\left(\prod_{m=2}^{M-1}\frac{1+h_m\sum\limits_{i=m}^{M+1} b_i}{1+h_m\sum\limits_{i=m}^{M} a_i}\frac{1+h_m\sum\limits_{i=m+1}^{M} a_i}{1+h_m\sum\limits_{i=m+1}^{M+1} b_i}\right)\left(\frac{1+h_M\sum\limits_{i=M}^{M+1} b_i}{1+h_M a_M}\frac{1+h_{M+1}b_{M+1}}{1+h_M b_{M+1}}\right)\right)\\
&= \log_2\left(\underbrace{\frac{1+h_1\sum\limits_{i=2}^{M} a_i}{1+h_1\sum\limits_{i=2}^{M+1} b_i}\frac{1+h_2\sum\limits_{i=2}^{M+1} b_i}{1+h_2\sum\limits_{i=2}^{M} a_i}}_{I_1}\left(\underbrace{\prod_{m=2}^{M-1}\frac{\left(1+h_m\sum\limits_{i=m+1}^{M} a_i\right)}{\left(1+h_m\sum\limits_{i=m+1}^{M+1} b_i\right)}\frac{\left(1+h_{m+1}\sum\limits_{i=m+1}^{M+1} b_i\right)}{\left(1+h_{m+1}\sum\limits_{i=m+1}^{M} a_i\right)}}_{I_2}\right)\underbrace{\left(\frac{1+h_{M+1}b_{M+1}}{1+h_M b_{M+1}}\right)}_{I_3}\right).
\end{aligned}
$$

[7] Z. Lin, H. Niu, K. An, Y. Wang, G. Zheng, S. Chatzinotas, and Y. Hu, "Refracting RIS-Aided Hybrid Satellite-Terrestrial Relay Networks: Joint Beamforming Design and Optimization," *IEEE Transactions on Aerospace and Electronic Systems*, vol. 58, no. 4, pp. 3717–3724, Aug. 2022.

[8] Z. Lin, K. An, H. Niu, Y. Hu, S. Chatzinotas, G. Zheng, and J. Wang, "SLNR-based Secure Energy Efficient Beamforming in Multibeam Satellite Systems," *IEEE Trans. Aerosp. Electron. Syst.*, pp. 1–4, 2022.

[9] X. Liu, X. B. Zhai, W. Lu, and C. Wu, "QoS-Guarantee Resource Allocation for Multibeam Satellite Industrial Internet of Things With NOMA," *IEEE Trans. Ind. Inform.*, vol. 17, no. 3, pp. 2052–2061, Mar. 2021.

[10] O. Kodheli, E. Lagunas, N. Maturo, S. K. Sharma, B. Shankar, J. F. M. Montoya, J. C. M. Duncan, D. Spano, S. Chatzinotas, S. Kisseleff, J. Querol, L. Lei, T. X. Vu, and G. Goussetis, "Satellite Communications in the New Space Era: A Survey and Future Challenges," *IEEE Commun. Surv. Tutor.*, vol. 23, no. 1, pp. 70–109, firstquarter, 2021.

[11] C. Zhang, C. Jiang, L. Kuang, J. Jin, Y. He, and Z. Han, "Spatial Spectrum Sharing for Satellite and Terrestrial Communication Networks," *IEEE Trans. Aerosp. Electron. Syst.*, vol. 55, no. 3, pp. 1075–1089, Jun. 2019.

[12] Q. Huang, M. Lin, W.-P. Zhu, S. Chatzinotas, and M.-S. Alouini, "Performance Analysis of Integrated Satellite-Terrestrial Multiantenna Relay Networks With Multiuser Scheduling," *IEEE Trans. Aerosp. Electron. Syst.*, vol. 56, no. 4, pp. 2718–2731, Aug. 2020.

[13] A. Wang, L. Lei, E. Lagunas, A. I. Pérez-Neira, S. Chatzinotas, and B. Ottersten, "NOMA-Enabled Multi-Beam Satellite Systems: Joint Optimization to Overcome Offered-Requested Data Mismatches," *IEEE Trans. Veh. Technol.*, vol. 70, no. 1, pp. 900–913, Jan. 2021.

[14] C. Han, L. Huo, X. Tong, H. Wang, and X. Liu, "Spatial Anti-Jamming Scheme for Internet of Satellites Based on the Deep Reinforcement Learning and Stackelberg Game," *IEEE Trans. Veh. Technol.*, vol. 69, no. 5, pp. 5331–5342, May 2020.

[15] H. Yang, Z. Xiong, J. Zhao, D. Niyato, Q. Wu, H. V. Poor, and M. Tornatore, "Intelligent Reflecting Surface Assisted Anti-Jamming Communications: A Fast Reinforcement Learning Approach," *IEEE Trans. Wireless Commun.*, vol. 20, no. 3, pp. 1963–1974, Mar. 2021.

[16] C. Han, A. Liu, H. Wang, L. Huo, and X. Liang, "Dynamic Anti-Jamming Coalition for Satellite-Enabled Army IoT: A Distributed Game Approach," *IEEE Internet Things J.*, vol. 7, no. 11, pp. 10 932–10 944, Nov., 2020.

[17] Y. Xu, Y. Xu, X. Dong, G. Ren, J. Chen, X. Wang, L. Jia, and L. Ruan, "Convert Harm Into Benefit: A Coordination-Learning Based Dynamic Spectrum Anti-Jamming Approach," *IEEE Trans. Veh. Technol.*, vol. 69, no. 11, pp. 13 018–13 032, Nov 2020.

[18] C. Han, A. Liu, L. Huo, H. Wang, X. Liang, and X. Tong, "Distributed Resource Management Framework for IoS Against Malicious Jamming," *IEEE Trans. Commun.*, vol. 69, no. 12, pp. 8271–8286, Dec. 2021.

[19] C. Han, A. Liu, K. An, H. Wang, G. Zheng, S. Chatzinotas, L. Huo, and X. Tong, "Satellite-assisted UAV Trajectory Control in Hostile Jamming Environments," *IEEE Trans. Veh. Technol.*, vol. 71, no. 4, pp. 3760 – 3775, Nov. 2022.

[20] Z. Yin, M. Jia, N. Cheng, W. Wang, F. Lyu, Q. Guo, and X. Shen, "UAV-Assisted Physical Layer Security in Multi-Beam Satellite-Enabled Vehicle Communications," *IEEE Trans. Intell. Transp. Syst.*, vol. 23, no. 3, pp. 2739–2751, Mar. 2022.

[21] Z. Yin, N. Cheng, T. H. Luan, and P. Wang, "Physical Layer Security in Cybertwin-Enabled Integrated Satellite-Terrestrial Vehicle Networks," *IEEE Trans. Veh. Technol.*, vol. 71, no. 5, pp. 4561–4572, May 2022.

[22] Z. Yin, N. Cheng, T. H. Luan, Y. Hui, and W. Wang, "Green Interference Based Symbiotic Security in Integrated Satellite-Terrestrial Communications," *IEEE Trans. Wireless Commun.*, vol. 21, no. 11, pp. 9962–9973, Nov. 2022.

[23] X. Yan, K. An, T. Liang, G. Zheng, Z. Ding, S. Chatzinotas, and Y. Liu, "The Application of Power-Domain Non-Orthogonal Multiple Access in Satellite Communication Networks," *IEEE Access*, vol. 7, pp. 63 531–63 539, 2019.

[24] L. Dai, B. Wang, Z. Ding, Z. Wang, S. Chen, and L. Hanzo, "A Survey of Non-Orthogonal Multiple Access for 5G," *IEEE Commun. Surv. Tutor.*, vol. 20, no. 3, pp. 2294–2323, thirdquarter 2018.

[25] Y. Liu, Z. Ding, M. Elkashlan, and H. V. Poor, "Cooperative Non-orthogonal Multiple Access With Simultaneous Wireless Information and Power Transfer," *IEEE J. Sel. Areas Commun.*, vol. 34, no. 4, pp. 938–953, Apr. 2016.

[26] M. B. Shahab, R. Abbas, M. Shirvanimoghaddam, and S. J. Johnson, "Grant-Free Non-Orthogonal Multiple Access for IoT: A Survey," *IEEE Commun. Surv. Tutor.*, vol. 22, no. 3, pp. 1805–1838, thirdquarter 2020.

[27] Y. Xu, B. Li, N. Zhao, Y. Chen, G. Wang, Z. Ding, and X. Wang, "Coordinated Direct and Relay Transmission With NOMA and Network Coding in Nakagami-m Fading Channels," *IEEE Trans. Commun.*, vol. 69, no. 1, pp. 207–222, Jan. 2021.

[28] J. Zhu, J. Wang, Y. Huang, F. Fang, K. Navaie, and Z. Ding, "Resource Allocation for Hybrid NOMA MEC Offloading," *IEEE Trans. Wireless Commun.*, vol. 19, no. 7, pp. 4964–4977, Jul. 2020.

[29] Z. Gao, A. Liu, and X. Liang, "The Performance Analysis of Downlink NOMA in LEO Satellite Communication System," *IEEE Access*, vol. 8, pp. 93 723–93 732, 2020.

[30] X. Zhu, C. Jiang, L. Kuang, N. Ge, and J. Lu, "Non-Orthogonal Multiple Access Based Integrated Terrestrial-Satellite Networks," *IEEE J. Sel. Areas Commun.*, vol. 35, no. 10, pp. 2253–2267, Oct. 2017.

[31] J. Kim and I. Lee, "Capacity Analysis of Cooperative Relaying Systems Using Non-Orthogonal Multiple Access," *IEEE Commun. Lett.*, vol. 19, no. 11, pp. 1949–1952, Nov. 2015.

[32] T. Qi, W. Feng, and Y. Wang, "Outage Performance of Non-orthogonal Multiple Access based Unmanned Aerial Vehicles Satellite Networks," *China Commun.*, vol. 15, no. 5, pp. 1–8, May 2018.

[33] F. Kara and H. Kaya, "On the Error Performance of Cooperative-NOMA With Statistical CSIT," *IEEE Commun. Lett.*, vol. 23, no. 1, pp. 128–131, Jan. 2019.

[34] L. Lv, Q. Ye, Z. Ding, Z. Li, N. Al-Dhahir, and J. Chen, "Multi-Antenna Two-Way Relay Based Cooperative NOMA," *IEEE Trans. Wireless Commun.*, vol. 19, no. 10, pp. 6486–6503, Oct. 2020.

[35] B. Wang, L. Dai, Z. Wang, N. Ge, and S. Zhou, "Spectrum and Energy-Efficient Beamspace MIMO-NOMA for Millimeter-Wave Communications Using Lens Antenna Array," *IEEE J. Sel. Areas Commun.*, vol. 35, no. 10, pp. 2370–2382, Oct. 2017.

[36] W. Wang, N. Zhao, L. Chen, X. Liu, Y. Chen, and D. Niyato, "UAV-Assisted Time-Efficient Data Collection via Uplink NOMA," *IEEE Trans. Commun.*, vol. 69, no. 11, pp. 7851–7863, Nov. 2021.

[37] W. Feng, J. Tang, N. Zhao, X. Zhang, X. Wang, K.-K. Wong, and J. A. Chambers, "Hybrid Beamforming Design and Resource Allocation for UAV-Aided Wireless-Powered Mobile Edge Computing Networks With NOMA," *IEEE J. Sel. Areas Commun.*, vol. 39, no. 11, pp. 3271–3286, Nov. 2021.

[38] W. Feng, N. Zhao, S. Ao, J. Tang, X. Zhang, Y. Fu, D. K. C. So, and K.-K. Wong, "Joint 3D Trajectory and Power Optimization for UAV-Aided mmWave MIMO-NOMA Networks," *IEEE Trans. Commun.*, vol. 69, no. 4, pp. 2346–2358, Apr. 2021.

[39] X. Zhang, Q. Gao, C. Gong, and Z. Xu, "User Grouping and Power Allocation for NOMA Visible Light Communication Multi-Cell Networks," *IEEE Commun. Lett.*, vol. 21, no. 4, pp. 777–780, Apr. 2017.

[40] W. Wu, X. Wang, F. Zhou, K.-K. Wong, C. Li, and B. Wang, "Resource Allocation for Enhancing Offloading Security in NOMA-Enabled MEC Networks," *IEEE Syst. J.*, vol. 15, no. 3, pp. 3789–3792, Jul. 2021.

[41] Z. Ding, Y. Liu, J. Choi, Q. Sun, M. Elkashlan, I. Chih-Lin, and H. V. Poor, "Application of Non-Orthogonal Multiple Access in LTE and 5G Networks," *IEEE Commun. Mag.*, vol. 55, no. 2, pp. 185–191, Feb. 2017.

[42] L. Lei, D. Yuan, C. K. Ho, and S. Sun, "Power and Channel Allocation for Non-Orthogonal Multiple Access in 5G Systems: Tractability and Computation," *IEEE Trans. Wireless Commun.*, vol. 15, no. 12, pp. 8580–8594, Dec. 2016.

[43] Y. Sun, D. W. K. Ng, Z. Ding, and R. Schober, "Optimal Joint Power and Subcarrier Allocation for Full-Duplex Multicarrier Non-Orthogonal Multiple Access Systems," *IEEE Trans. Commun.*, vol. 65, no. 3, pp. 1077–1091, Mar. 2017.

[44] H. Zhang, N. Yang, K. Long, M. Pan, G. K. Karagiannidis, and V. C. M. Leung, "Secure Communications in NOMA System: Subcarrier Assignment and Power Allocation," *IEEE J. Sel. Areas Commun.*, vol. 36, no. 7, pp. 1441–1452, 2018.

[45] Z. Lin, M. Lin, J. Wang, T. de Cola, and J. Wang, "Joint Beamforming and Power Allocation for Satellite-Terrestrial Integrated Networks With Non-Orthogonal Multiple Access," *IEEE J. Sel. Top. Signal Process.*, vol. 13, no. 3, pp. 657–670, Jun. 2019.

[46] H. Zhang, B. Di, Z. Chang, X. Liu, L. Song, and Z. Han, "Equilibrium Problems With Equilibrium Constraints Analysis for Power Control and User Scheduling in NOMA Networks," *IEEE Trans. Veh. Technol.*, vol. 69, no. 5, pp. 5467–5480, May 2020.

[47] M. Zhang, H. Lu, F. Wu, and C. W. Chen, "NOMA-Based Scalable Video Multicast in Mobile Networks With Statistical Channels," *IEEE Trans. Mob. Comput.*, vol. 20, no. 6, pp. 2238–2253, Jun., 2021.

[48] Y. Yin, M. Liu, G. Gui, H. Gacanin, H. Sari, and F. Adachi, "Cross-Layer Resource Allocation for UAV-Assisted Wireless Caching Networks With NOMA," *IEEE Trans. Veh. Technol.*, vol. 70, no. 4, pp. 3428–3438, Apr. 2021.

[49] J. Chu and X. Chen, "Robust Design for Integrated Satellite–Terrestrial Internet of Things," *IEEE Internet Things J.*, vol. 8, no. 11, pp. 9072–9083, Jun. 2021.

[50] S. Liao, J. Jiao, S. Wu, R. Lu, and Q. Zhang, "Age-Optimal Power Allocation Scheme for NOMA-based S-IoT Downlink Network," in *ICC 2021 - IEEE International Conference on Communications*, Jun. 2021, pp. 1–6.

[51] X. Zhou, K. Ying, Z. Gao, Y. Wu, Z. Xiao, S. Chatzinotas, J. Yuan, and B. Ottersten, "Active Terminal Identification, Channel Estimation, and Signal Detection for Grant-Free NOMA-OTFS in LEO Satellite Internet-of-Things," *IEEE Trans. Wireless Commun.*, pp. 1–1, 2022.

[52] K. An, M. Lin, and T. Liang, "On the Performance of Multiuser Hybrid Satellite-Terrestrial Relay Networks With Opportunistic Scheduling," *IEEE Commun. Lett.*, vol. 19, no. 10, pp. 1722–1725, Oct. 2015.

[53] K. An, T. Liang, G. Zheng, X. Yan, Y. Li, and S. Chatzinotas, "Performance Limits of Cognitive-Uplink FSS and Terrestrial FS for Ka-Band," *IEEE Trans. Aerosp. Electron. Syst.*, vol. 55, no. 5, pp. 2604–2611, Oct. 2019.

[54] L. You, K. X. Li, J. Wang, X. Gao, X. G. Xia, and B. Ottersten, "Massive MIMO Transmission for LEO Satellite Communications," *IEEE J. Sel. Areas Commun.*, vol. 38, no. 8, pp. 1851–1865, Aug., 2020.

[55] K. An, M. Lin, J. Ouyang, and W.-P. Zhu, "Secure Transmission in Cognitive Satellite Terrestrial Networks," *IEEE J. Sel. Areas Commun.*, vol. 34, no. 11, pp. 3025–3037, Nov 2016.

[56] X. Yan, H. Xiao, C. Wang, K. An, A. T. Chronopoulos, and G. Zheng, "Performance Analysis of NOMA-Based Land Mobile Satellite Networks," *IEEE Access*, vol. 6, pp. 31 327–31 339, 2018.

[57] M. Zeng, A. Yadav, O. A. Dobre, G. I. Tsiropoulos, and H. V. Poor, "Capacity Comparison Between MIMO-NOMA and MIMO-OMA With Multiple Users in a Cluster," *IEEE J. Sel. Areas Commun.*, vol. 35, no. 10, pp. 2413–2424, 2017.

[58] O. L. A. López, H. Alves, and M. Latva-Aho, "Distributed Rate Control in Downlink NOMA Networks With Reliability Constraints," *IEEE Trans. Wireless Commun.*, vol. 18, no. 11, pp. 5410–5423, Nov. 2019.

[59] P. Parida and S. S. Das, "Power allocation in OFDM based NOMA systems: A DC programming approach," in *2014 IEEE Globecom Workshops (GC Wkshps)*, 2014, pp. 1026–1031.

[60] R. Zhang, X. Pang, J. Tang, Y. Chen, N. Zhao, and X. Wang, "Joint Location and Transmit Power Optimization for NOMA-UAV Networks via Updating Decoding Order," *IEEE Wireless Commun. Lett.*, vol. 10, no. 1, pp. 136–140, Jan. 2021.

[61] B. Di, L. Song, and Y. Li, "Sub-Channel Assignment, Power Allocation, and User Scheduling for Non-Orthogonal Multiple Access Networks," *IEEE Trans. Wireless Commun.*, vol. 15, no. 11, pp. 7686–7698, Nov. 2016.

[62] M. Elhattab, M. A. Arfaoui, C. Assi, and A. Ghrayeb, "RIS-Assisted Joint Transmission in a Two-Cell Downlink NOMA Cellular System," *IEEE J. Sel. Areas Commun.*, vol. 40, no. 4, pp. 1270–1286, Apr. 2022.

[63] J. Chen, Q. Wu, Y. Xu, N. Qi, X. Guan, Y. Zhang, and Z. Xue, "Joint Task Assignment and Spectrum Allocation in Heterogeneous UAV Communication Networks: A Coalition Formation Game-Theoretic Approach," *IEEE Trans. Wireless Commun.*, vol. 20, no. 1, pp. 440–452, Jan. 2021.